KAERI/TR-3592/2008

기술보고서

# Description of Freon Thermal Hydraulic Experimental Loop (FTHEL) and Its Application

## 프레온 열수력 실험 장치의 계통 설명 및 활용



한 국 원 자 력 연 구 원

# 제 출 문

한국원자력연구원장 귀하

본 보고서를 2008년도 원자력 기술개발사업 “핵심 열수력 개별현상 고정밀 실험”과제 (과제책임자: 송철화)의 기술보고서로 제출합니다.

2008. 6.


주 저 자: 강경호
공 저 자: 신창환
추연준
윤영중
박종국
김복득
문상기
천세영
송철화
백원필

# SUMMARY

## I. TITLE

Description of Freon Thermal Hydraulic Experimental Loop (FTHEL) and Its Application

## II. CONTENTS

Freon Thermal Hydraulic Experimental Loop (FTHEL) is being operated at the Korea Atomic Energy Research Institute (KAERI). The FTHEL is used to investigate a thermal mixing and a critical heat flux (CHF) performance in 5x5 rod bundles. The Freon, HFC-134a, is used as working fluid medium. The FTHEL consists of a closed hydraulic loop with main circulation pumps, pre-heaters, test section, direct current (DC) power supply, condensers and coolers. The system was designed with operating limits of 4.5 MPa and 150 $^{o}$C. Flow in the loop is provided by two non-seal canned motor pumps in a series arrangement. The series arrangement of the main circulation pumps provides a total developed head of 100 m. System pressure is controlled by accumulator using compressed nitrogen gas as working fluid. A pair of pre-heaters adjusts the inlet temperature of fluid at the test section. The vapor generated in the test section is condensed in the shell-tube type condensers and cooled in the same type coolers. The power to the test section is supplied from a 60 V x 12000 A, DC source.

Experiments have been performed to construct the CHF data base under the various experimental conditions using the FTHEL. The primary objectives of the experiments are to investigate the CHF performance according to the design of spacer grid, the effect of unheated rods and the heat transfer characteristics at near- and supercritical pressure conditions.

# 요 약 문

## I. 제 목

프레온 열수력 실험장치의 계통 설명 및 활용

## II. 내 용

한국원자력연구원에서는 프레온 열수력 실험 장치(FTHEL: Freon Theraml Hydraulic Experimental Loop)를 운영하고 있다. 프레온 열수력 실험 장치는 프레온 냉매(HFC-134a)를 사용하여 5x5 봉다발에서 열혼합과 임계열유속 (CHF: Critical Heat Flux) 성능 평가를 위한 실험 수행에 활용된다. 프레온 열수력 실험 장치는 주냉각펌프, 가압기, 예열기, 시험대, 응축기 및 열교환기로 구성되어 있다. 실험 장치는 스테인레스 스틸로 제작되었으며, 실험 장치의 최대 운저 허용 압력과 온도는 각각 4.5 MPa, 150 $^{o}$C이다. 주냉각재 펌프는 non-seal canned motor 펌프로서 펌프 두 대를 직렬로 설치하여 100m의 최대 수두로 냉각재를 순환시킨다. 계통 압력은 질소 가스를 사용하는 accumulator를 이용하여 제어한다. 예열기는 시험대의 입구온도를 조절하는 장치이며, 응축기는 시험대에서 생성된 증기를 응축하는 장치로서 쉘튜브형의 개별 응축기의 용량은 40 kW로 두 개를 사용하여 총 용량은 80 kW이다. 시험대에서 가열된 냉각수를 냉각시켜 시험대 입구에서의 유체온도를 일정하게 유지시키기 위한 열교환기는 두 대가 병렬로 설치되어 있으며, 열전달 조절 범위를 넓히기 위하여 우회 유로를 설치하였다. 프레온 열수력 실험 장치의 전원 공급 장치는 전압이 최고 60 V까지 공급되고 전류는 최고 12000 A까지 제공되는 직류전원장치이다.

프레온 열수력 실험 장치를 이용하여 광범위한 실험 조건에서 임계열유속 데이터베이스를 구축하기 위한 실험을 수행하였다. 지지격자의 형상에 따른 임계열유속의 특성과 성능 평가를 위한 실험을 수행하였으며, 5x5 봉다발 내에 비가열봉을 삽입하여 비균일 출력분포 효과에 대한 특성 실험 및 초임계압 근처 임계열유속 실험과 초임계압 압력 천이 열전달 실험을 수행하여 다양한 원자로 운전 조건에 대한 임계열유속과 열전달 특성을 분석하였다.

# List of Contents

## List of Tables

## List of Figures

# 1. Introduction

Critical heat flux (CHF) is an important thermal hydraulic parameter that limits the available power during normal operating condition of the light water reactor (LWR). Because the CHF results in a sudden rise in the fuel temperature, the reactor core and nuclear fuel should be designed with an appropriate margin so that the heat flux on the surface of a fuel rod does not exceed the CHF during any condition of a normal operation. As one of the most important limiting factors for the integrity of the fuel rod, the CHF database should be accurately compiled to avoid an excessive conservation or uncertainties in CHF estimations.

A fuel assembly of the nuclear reactors includes the spacer grids for supporting the fuel assembly. In most operating nuclear reactors, the spacer grids with mixing vanes have been adopted to improve the homogeneity of local properties inside the subchannel between the fuel rods. Besides the existence of the spacer grids with mixing vanes, a fuel assembly includes the unheated rods to insert control rods or in-core detectors as well as to replace damaged fuel rods during the operation. These unheated rods may change a radial power distribution and eventually affect on the local thermal hydraulic properties in the sub channels. These unique hydrodynamic characteristics involved in rod bundle geometry can affect the CHF performance in a fuel assembly of the nuclear reactors, which is the primary need for the CHF experiments in the bundle geometry.

Most of the CHF experiments have been carried out using water as a working fluid because the CHF in water cooled nuclear reactors is one of the most important thermal hydraulic parameters limiting the available power. However, it is not easy to perform the water CHF experiments under the thermal hydraulic conditions of nuclear reactors, i.e., high pressures and high temperatures. Especially, the CHF experiments for complex geometries such as nuclear fuel bundles require large amounts of electrical power and a large scale facility. In order to reduce the cost and technical difficulties of the water CHF experiments, Freon fluids such as HCFC-123, HFC-134a, etc. have been frequently used as working fluids because of their lower latent heat of vaporization and lower critical pressure when compared with water. For a practical application to the nuclear industry, the CHF data from the Freon experiments is well known to be convertible into water-equivalent data with a fluid-to-fluid modeling technique[1].

Freon Thermal Hydraulic Experimental Loop (FTHEL) is being operated at the Korea Atomic Energy Research Institute (KAERI). The FTHEL is used to investigate a thermal mixing and a critical heat flux (CHF) performance in 5x5 rod bundles. The Freon, HFC-134a, is used as working fluid medium. The FTHEL consists of a closed hydraulic loop with main circulation pumps, pre-heaters, test section, direct current (DC) power supply, condensers and coolers. The system was designed with operating limits of 4.5 MPa and 150 $^{o}$C. Experiments have been performed to construct the CHF data base under the various experimental conditions using the FTHEL. The primary objectives of the experiments are to investigate the CHF performance according to the design of spacer grid, the effect of unheated rods and the heat transfer characteristics at near- and supercritical pressure conditions. In this report, detailed design specification of the FTHEL facility and its application are summarized.

## 2. Design Specification of FTHEL Facility

The FTHEL facility consists of a closed hydraulic loop with two non-seal canned motor pump connected in a series, a flow-meter, two pre-heaters, an inlet throttling valve, a test section, a condensing and cooling system. Figure 2-1 shows the schematic diagram of the FTHEL facility. The Freon, HFC-134a, is used as the working fluid medium. The system was designed with operating limits of 4.5 MPa and 150 $^{o}$C.

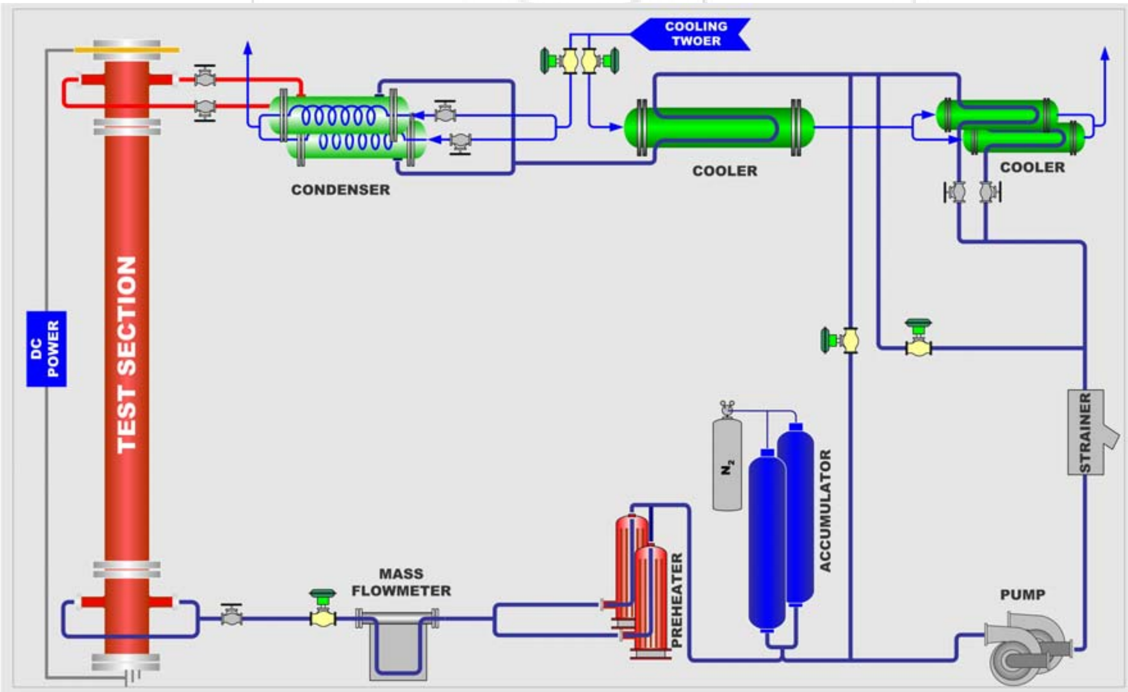


Figure 2-1. Schematic diagram of Freon Thermal Hydraulic Experimental Loop (FTHEL)

## 2.1. Main Circulation Pump

Flow in the loop is provided by two non-seal canned motor pumps in a series arrangement, manufactured by Halla Industrial Corporation. Each pump delivers 910 liter/min against a head of 50 m water for 18 $^{o}$C. The series arrangement provides a total developed head of 100 m. The flow rate is represented as an rpm of pumps controlled by each inverter and an inlet throttling valve. A photograph of main pumps is shown in Figure 2-2.


Figure 2-2. Photograph of main circulation pump

## 2.2. Pressurizer

System pressure is controlled by a pair of accumulators using compressed nitrogen gas as a working fluid. Nitrogen gas is isolated from Freon by Buna-N bladder in an accumulator vessel. The compressed nitrogen gas is supplied from nitrogen storage tank to increase system pressure, and to the contrary, the nitrogen gas is vented from accumulator to decrease system pressure. In this loop, two accumulators are connected in a parallel arrangement. The design pressure and temperature of the accumulator are 7.0 MPa and 80 $^{o}$C. A photograph of accumulators is shown in Figure 2-3.


Figure 2-3. Photograph of pressurizer

## 2.3. Pre-heater

Two pre-heaters are used to control the inlet temperature at the test section. The capacity of 25 kW for each pre-heater is controlled by SCR (Silicon Controlled Rectifier) and the temperature is maintained by PID (Proportional Integral Differential) controller. The photograph of pre-heater is shown in Figure 2-4.

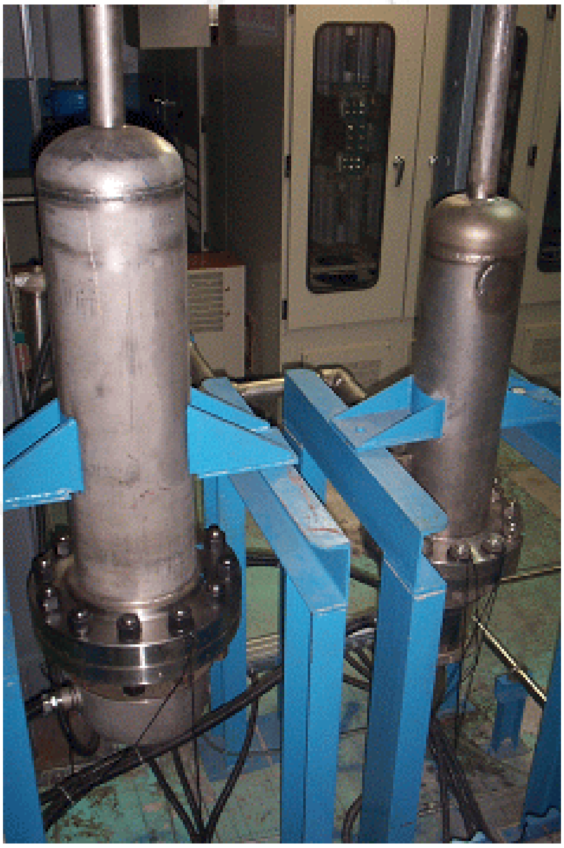

Figure 2-4. Photograph of pre-heater

## 2.4. Condenser

The vapor generated in a test section is condensed in two condenser of shell-tube type connected in parallel. The capacity of each condenser is 40 kW and the design pressure is 7.0 MPa. The photograph of condenser is shown in Figure 2-5.

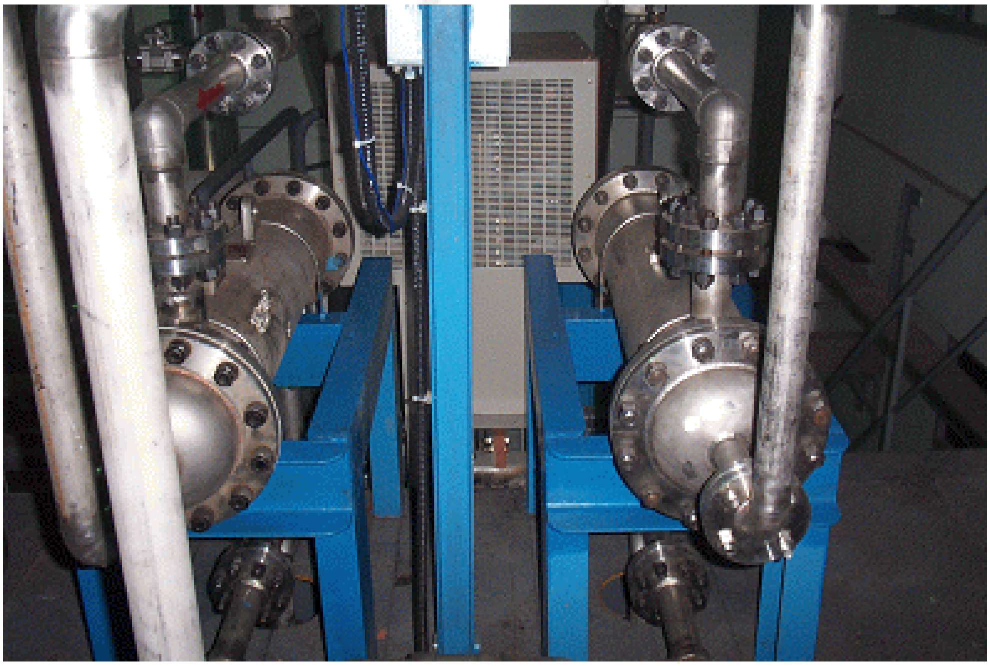

Figure 2-5. Photograph of condenser

## 2.5. Heat Exchanger

Three heat exchangers are used for cooling of working fluid heated in test section. Heat exchangers are shell-tube type and consists of two heat exchangers having a total capacity of 300 kW connected in parallel and a heat exchanger of 200 kW capacity connected in series arrangement with the others. The photograph of heat exchanger is shown in Figure 2-6.

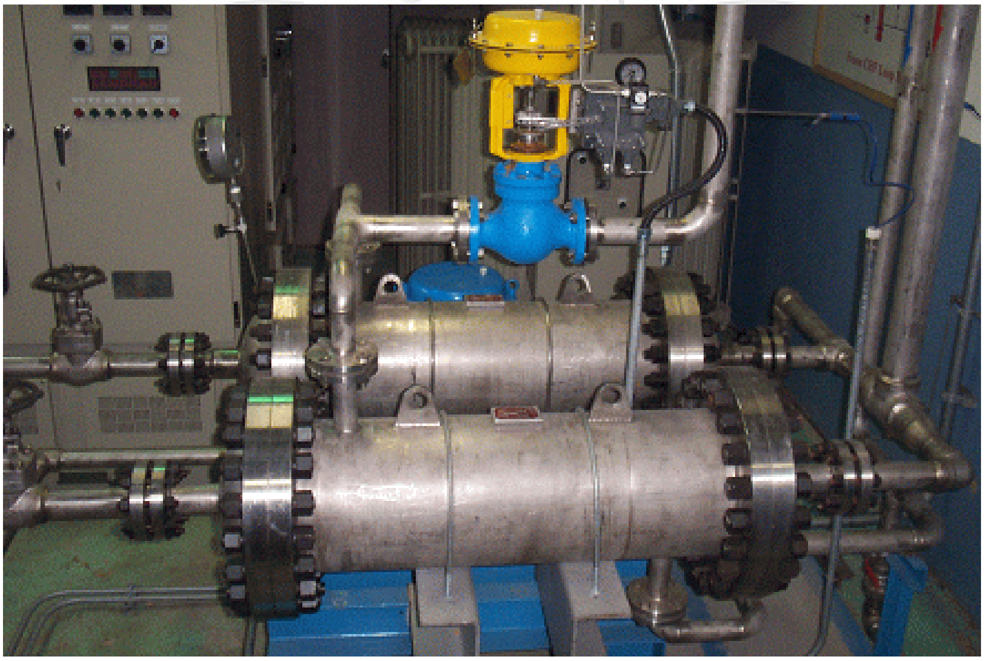

Figure 2-6. Photograph of heat exchanger

## 2.6. Electrical System

In the FTHEL, a DC (Direct Current) power is used for the electrical power to the heater rods. The DC power supply system includes a potential transformer to drop the electric potential from an AC (Alternating Current) input to a pertinent DC voltage. A reduced voltage is rectified, and the ripple is eliminated by a capacitor or LC filter circuit. Besides, the voltage conditioning circuit is added to generate the more stable DC power voltage. The power of FTHEL is supplied up to 720 kW by the DC power supply of maximum 60 V for voltage and maximum 12000 amperes for a current.

## 2.7. Measurement System

The major instrumentations required for the CHF test are described in this section. They are as follows:

○ Fluid temperature at the inlet and outlet of test section,
○ Pressure at the inlet and outlet of the test section,
○ Test section inlet mass flow rate
○ Total power to the test section

Fluid temperature at the inlet and outlet of the test section are measured by calibrated platinum resistive thermometers (RTD). And also T-type thermocouples of Copper-Constantan are installed for complementary measurement. The thermocouples are connected to the data acquisition system and processed by the data acquisition system.

Pressure measurements are made at the inlet and the outlet of the test section and the loop of the test facility. Smart type pressure transmitters manufactured by Rosemount are used for the measurement of pressure. Flow rate is measured with U-tube type mass flow meter having accuracy of ±0.2%, which was manufactured by Micro Motion.

The DC power applied to the test section is measured by means of voltage and current readings. Voltage drops are directly measured by an integral voltmeter by means of two copper wires connected at both ends of the copper power clamps in the test section. For measuring the electric current, a shunt with ±0.5 % of accuracy is installed between the main power line and the test section, and it measures the DC to 15000 amperes.

## 2.8. Measurement Uncertainties

Every measurement always includes error which results in a difference between the measured value and the true value. The difference between the measured value and the true value is the total measurement error. Since the true value or the error is unknown and unknowable, its limits must be estimated at a given confidence. This estimate is called the uncertainty. In 1993, the International Organization for Standardization (ISO) published the "Guide to the Expression of Uncertainty in Measurement (GUM)" in the name of seven international organizations, which formally established general rules for evaluating and expressing uncertainty in measurement. This guide was corrected and reprinted in 1995 and usually referred to simply as the GUM[2].

The uncertainties of the measurements were estimated from the calibration of the sensors and the accuracy of the equipments according to the ISO GUM method with a confidence level of 95 %. The evaluated maximum uncertainties of the pressures, flow rates, and temperatures are less than ±0.25 %, ±0.6 % and ±0.7 $^{o}$C of the readings in the range od interest, respectively. The uncertainty of the power calculated from the voltage and current applied to the heat rod bundle is always less than ±1.8 % of readings.

# 3. Experimental Procedure

Experimental procedure which includes the test operation and the descriptions of the data acquisition system is explained below.

## 3.1. Operation

Before starting a set of experiments, a heat balance test under single phase condition is carried out to estimate the heat loss from the test section and to check a proper working of the test section instrumentation. In the heat balance tests, under the specific test conditions of test section outlet pressure, inlet temperature, and mass flow rate, total power applied to the heater rods is compared with the enthalpy rise of fluid through the test section. The parameter for the estimation of the heat balance is defined as follows:

$$\eta = \frac{Q_T}{GA_f(h_e - h_i)} \times 100$$

Where $Q_T$ = total power to the heater rods (kW)

$G$ = mass flux at the test section (kg/(m$^2$s))

$A_f$ = flow area at the heated region

$h_e$= enthalpy at the test section outlet (kJ/kg)

$h_i$= enthalpy at the test section inlet (kJ/kg)

If the $\eta$ is within 100±3 %, the overall operation of the test loop is considered as to be pertinent and then the CHF test will be started.

These tests will be taken when the test loop has reached equilibrium after initial heat up. Nominal conditions of the heat balance test are the exit pressure of 2500 kPa, the inlet temperature of 50 $^{o}C$, the mass flux of 2000 kg/($m^2$s), and the total power of 150 kW. The nominal conditions for the heat balance test can be changed according to daily circumstances such as the minimum achievable inlet temperature and daily test condition. After achieving the equilibrium state, the heat balance test data for about 400 sec are recorded and analyzed.

The CHF experiments are performed by maintaining the following system conditions constant: test section outlet pressure, inlet temperature, and mass flow rate. In the CHF test, the power is applied to the heater rod bundle of the test section and then increased gradually in small steps (usually less than 0.2 % increments of preceding power level at near the estimated CHF condition) while the system conditions are kept constant. The CHF condition is defined as a sharp and continuous rise of the wall temperatures on the heater rod. The power is increased until a temperature excursion is observed by one or more of the thermocouples embedded inside the heater rods. The amount of the excursion is approximately 35 $^{o}C$. The CHF detection and protection system scans continuously the temperature signals from all the thermocouples installed in the heater rods. When the wall temperature reaches the pre-determined set point of saturation temperature under system pressure plus 35 $^{o}C$, the DC power to the heater rod is automatically decreased or tripped by the power run down/trip system.

When a CHF point is observed, the following measurements are automatically recorded, and the final CHF data are generated using post-processing program.

- Test section inlet and outlet pressure
- Test section inlet and outlet fluid temperature
- Test section inlet mass flow rate
- Test section voltage and current
- Heater rod temperatures
- Rod(s) experiencing CHF
- Average heat flux at CHF condition

## 3.2. Data Acquisition System

The data acquisition system measures analog signals from various instruments, generates alarm signals, and controls the heater power in case of emergency in order to protect the heater rods. The data acquisition system of the FTHEL consists of HP 3852a Data Acquisition/Control Unit and a personal computer. The personal computer sends commands to the HP 3852a data acquisition system through HP VEE program, and converts the signals measured by the HP 3852a into physical quantities. The personal computer and HP 3852a are connected by GPIB (General Purpose Interface Bus) interface, and can exchange various commands and signals with each other.

Table 3-1 shows the configuration of the HP 3852a data acquisition system. Figures 3-1 and 3-2 show the HP VEE programs where the main loop and heater wall temperature measurements are shown. Table 3-2 shows the configuration of the data acquisition system for the main loop measurements except for the heater wall temperature. Table 3-3 shows the configuration of the data acquisition system for the heater wall temperature measurements, serial number of heater rods, and subchannel number where the wall temperature is measured. Table 3-4 shows the emergency signals to control the heater power in case of CHF occurrence, and the alarm signals to protect the main coolant pumps.

Table 3-1. HP 3852a data acquisition system

| Frame/Slot | Model No. | Technical Specification | Used Channels | Remarks |
|---|---|---|---|---|
| Main frame | HP 3852a | Data Acquisition/Control Unit | | |
| Slot 0 | 44701A | 5 1/2 Digit Integrating Voltmeter | | |
| Slot 1 | 44705A | 20ch Relay Multiplexer | 100-112 | 13 EA (Voltage) |
| Slot 2 | 44708A | 20ch Relay Multiplexer with T/C Compensation | 200-208 | 9 EA (T-type T/C) |
| | | | 212-219 | 8 EA (K-type T/C) |
| Slot 3 | 44708A | 20ch Relay Multiplexer with T/C Compensation | 300-319 | 20 EA (K-type T/C) |
| Slot 4 | 44708A | 20ch Relay Multiplexer with T/C Compensation | 400-419 | 20 EA (K-type T/C) |
| Slot 5 | 44708A | 20ch Relay Multiplexer with T/C Compensation | 500-515 | 16 EA (K-type T/C) |
| Slot 6 | 44705A | 20ch Relay Multiplexer | - | - |
| Slot 7 | 44727A | 4ch Voltage/Current DAC | 700-702 | 3 EA (Protection system) |

Table 3-2. Main loop instrumentations

| DAS Ch. No. | Instrument Tag No. | Span | Output Signal | Description |
|---|---|---|---|---|
| 100 | PT-01 | 0 ~ 5000 kPa | 1 ~ 5 V | Pressure at MCP outlet |
| 101 | FT-01 | 0 ~ 725.75 kg/min | 1 ~ 5 V | Mass flow rate |
| 102 | PT-04 | 0 ~ 5000 kPa | 1 ~ 5 V | Pressure at pre-heater outlet |
| 103 | PT-05 | 0 ~ 5000 kPa | 1 ~ 5 V | Pressure at test section inlet |
| 104 | PT-06 | 0 ~ 5000 kPa | 1 ~ 5 V | Pressure at test section outlet |
| 105 | PT-07 | 0 ~ 5000 kPa | 1 ~ 5 V | Pressure at condenser outlet |
| 106 | DPT-02 | 0 ~ 40 kPa | 1 ~ 5 V | Diff. pressure at strainer |
| 107 | PT-09 | 0 ~ 5000 kPa | 1 ~ 5 V | Pressure at MCP inlet |
| 108 | DPT-01 | -60 ~ 60 kPa | 1 ~ 5 V | Diff. pressure at test section |
| 109 | V | 0 ~ 70 V | 1 ~ 5 V | Test section voltage |
| 110 | I01 | 0 ~ 15000 A | 0 ~ 50 mV (1 ~ 5 V) | Test section current |
| 111 | RTD-IN | 0 ~ 150 $^{o}$C | 1 ~ 5 V | Test section inlet (RTD) |
| 112 | RTD-EX | 0 ~ 150 $^{o}$C | 1 ~ 5 V | Test section outlet (RTD) |
| 200 | TE-01 | 0 ~ 200 $^{o}$C | T-type T/C | MCP outlet (T-type T/C) |
| 201 | TE-02 | 0 ~ 200 $^{o}$C | T-type T/C | Flowmeter outlet (T-type T/C) |
| 202 | TE-03 | 0 ~ 200 $^{o}$C | T-type T/C | Test section inlet (T-type T/C) |
| 203 | TE-04 | 0 ~ 200 $^{o}$C | T-type T/C | Test section outlet (T-type T/C) |
| 204 | TE-05 | 0 ~ 200 $^{o}$C | T-type T/C | Condenser 1 outlet (T-type T/C) |
| 205 | TE-06 | 0 ~ 200 $^{o}$C | T-type T/C | Condenser 2 outlet (T-type T/C) |
| 206 | TE-07 | 0 ~ 200 $^{o}$C | T-type T/C | Condenser outlet (T-type T/C) |
| 207 | TE-08 | 0 ~ 200 $^{o}$C | T-type T/C | Cooler outlet (T-type T/C) |
| 208 | TE-09 | 0 ~ 200 $^{o}$C | T-type T/C | Strainer inlet (T-type T/C) |

Table 3-3. Wall temperature instrumentations (1/2)

| DAS Ch. No. | Instrument Tag No. (-) | Rod No.(-) | Heater Serial No. (-) | T/C No.(-) | Subchannel No. (-) | Remark |
|---|---|---|---|---|---|---|
| 212 | TW-01 | 1 | N1M-S11 | T/C 1 | 2 | |
| 213 | TW-02 | | | T/C 2 | 7 | |
| 214 | TW-03 | | | T/C 3 | 6 | |
| 215 | TW-04 | | | T/C 4 | 1 | |
| 216 | TW-05 | 2 | N1M-S03 | T/C 1 | 3 | |
| 217 | TW-06 | | | T/C 2 | 8 | |
| 218 | TW-07 | | | T/C 3 | 7 | |
| 219 | TW-08 | | | T/C 4 | 2 | |
| 300 | TW-09 | 3 | N1M-S04 | T/C 1 | 4 | |
| 301 | TW-10 | | | T/C 2 | 9 | |
| 302 | TW-11 | | | T/C 3 | 8 | |
| 303 | TW-12 | | | T/C 4 | 3 | |
| 304 | TW-13 | 4 | N1M-S01 | T/C 1 | 5 | |
| 305 | TW-14 | | | T/C 2 | 10 | |
| 306 | TW-15 | | | T/C 3 | 9 | |
| 307 | TW-16 | | | T/C 4 | 4 | |
| 308 | TW-17 | 5 | N1M-S06 | T/C 1 | 10 | |
| 309 | TW-18 | | | T/C 2 | 15 | |
| 310 | TW-19 | | | T/C 3 | 14 | |
| 311 | TW-20 | | | T/C 4 | 9 | |
| 312 | TW-21 | 6 | N1M-S05 | T/C 1 | 15 | |
| 313 | TW-22 | | | T/C 2 | 20 | |
| 314 | TW-23 | | | T/C 3 | 19 | |
| 315 | TW-24 | | | T/C 4 | 14 | |
| 316 | TW-25 | 7 | N1M-S10 | T/C 1 | 20 | |
| 317 | TW-26 | | | T/C 2 | 25 | |
| 318 | TW-27 | | | T/C 3 | 24 | |
| 319 | TW-28 | | | T/C 4 | 19 | |
| 400 | TW-29 | 8 | N1M-S07 | T/C 1 | 19 | |
| 401 | TW-30 | | | T/C 2 | 24 | |
| 402 | TW-31 | | | T/C 3 | 23 | |
| 403 | TW-32 | | | T/C 4 | 18 | |

Table 3-3. Wall temperature instrumentations (2/2)

| DAS Ch. No. | Instrument Tag No. (-) | Rod No.(-) | Heater Serial No. (-) | T/C No.(-) | Subchannel No. (-) | Remark |
|---|---|---|---|---|---|---|
| 404 | TW-33 | 9 | N1M-S13 | T/C 1 | 18 | |
| 405 | TW-34 | | | T/C 2 | 23 | |
| 406 | TW-35 | | | T/C 3 | 22 | |
| 407 | TW-36 | | | T/C 4 | 17 | |
| 408 | TW-37 | 10 | N1M-S08 | T/C 1 | 17 | |
| 409 | TW-38 | | | T/C 2 | 22 | |
| 410 | TW-39 | | | T/C 3 | 21 | |
| 411 | TW-40 | | | T/C 4 | 16 | |
| 412 | TW-41 | 11 | N1M-S09 | T/C 1 | 12 | |
| 413 | TW-42 | | | T/C 2 | 17 | |
| 414 | TW-43 | | | T/C 3 | 16 | |
| 415 | TW-44 | | | T/C 4 | 11 | |
| 416 | TW-45 | 12 | N1M-S02 | T/C 1 | 7 | |
| 417 | TW-46 | | | T/C 2 | 12 | |
| 418 | TW-47 | | | T/C 3 | 11 | |
| 419 | TW-48 | | | T/C 4 | 6 | |
| 500 | TW-49 | 13 | N1H-L01 | T/C 1 | 8 | |
| 501 | TW-50 | | | T/C 2 | 13 | |
| 502 | TW-51 | | | T/C 3 | 12 | |
| 503 | TW-52 | | | T/C 4 | 7 | |
| 504 | TW-53 | 14 | N1H-L03 | T/C 1 | 9 | |
| 505 | TW-54 | | | T/C 2 | 14 | |
| 506 | TW-55 | | | T/C 3 | 13 | |
| 507 | TW-56 | | | T/C 4 | 8 | |
| 508 | TW-57 | 15 | N1H-L05 | T/C 1 | 14 | |
| 509 | TW-58 | | | T/C 2 | 19 | |
| 510 | TW-59 | | | T/C 3 | 18 | |
| 511 | TW-60 | | | T/C 4 | 13 | |
| 512 | TW-61 | 16 | N1H-L04 | T/C 1 | 13 | |
| 513 | TW-62 | | | T/C 2 | 18 | |
| 514 | TW-63 | | | T/C 3 | 17 | |
| 515 | TW-64 | | | T/C 4 | 12 | |

Table 3-4. Protection signals for heater and main coolant pump

| DAS Ch. No. | Instrument Tag No. | Output Signal | Description |
|---|---|---|---|
| 700 | CHF1 | 0~10 V | ACB trip (heater power trip) |
| 701 | CHF2 | 0~10 V | IVR voltage decrease<br>(heater power decrease) |
| 702 | PUMP | 0~10 V | Alarm for MCP |

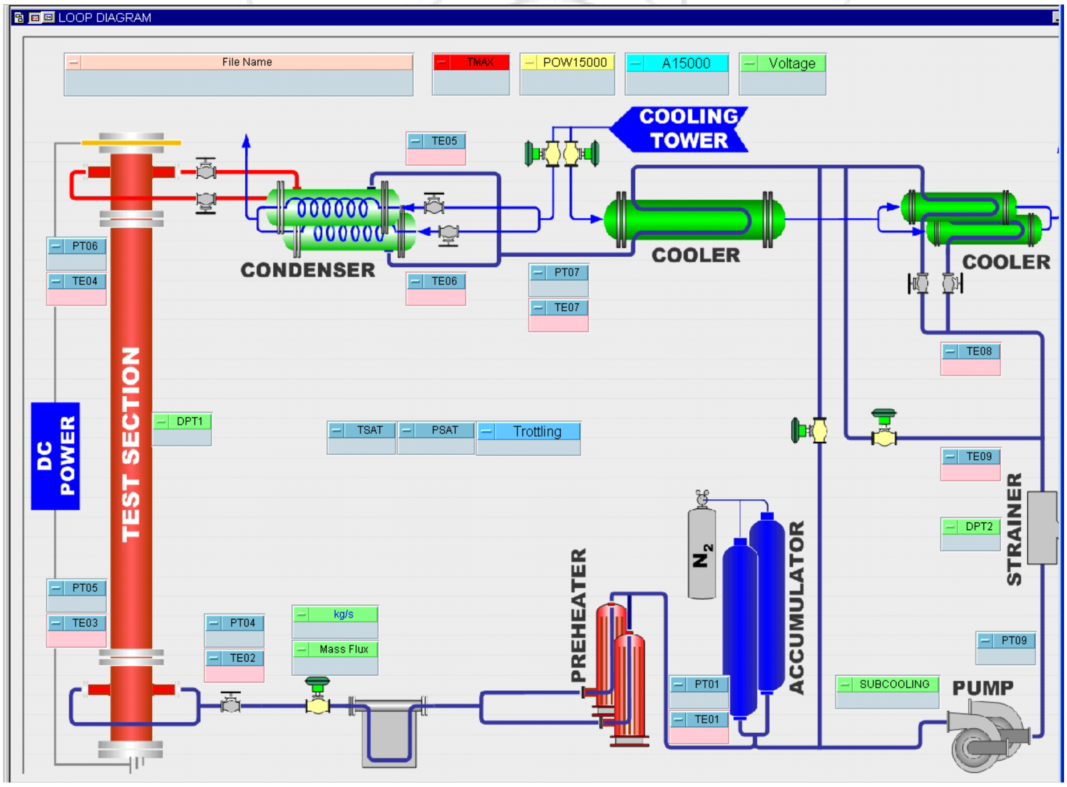


Figure 3-1. HP VEE programs showing the main loop

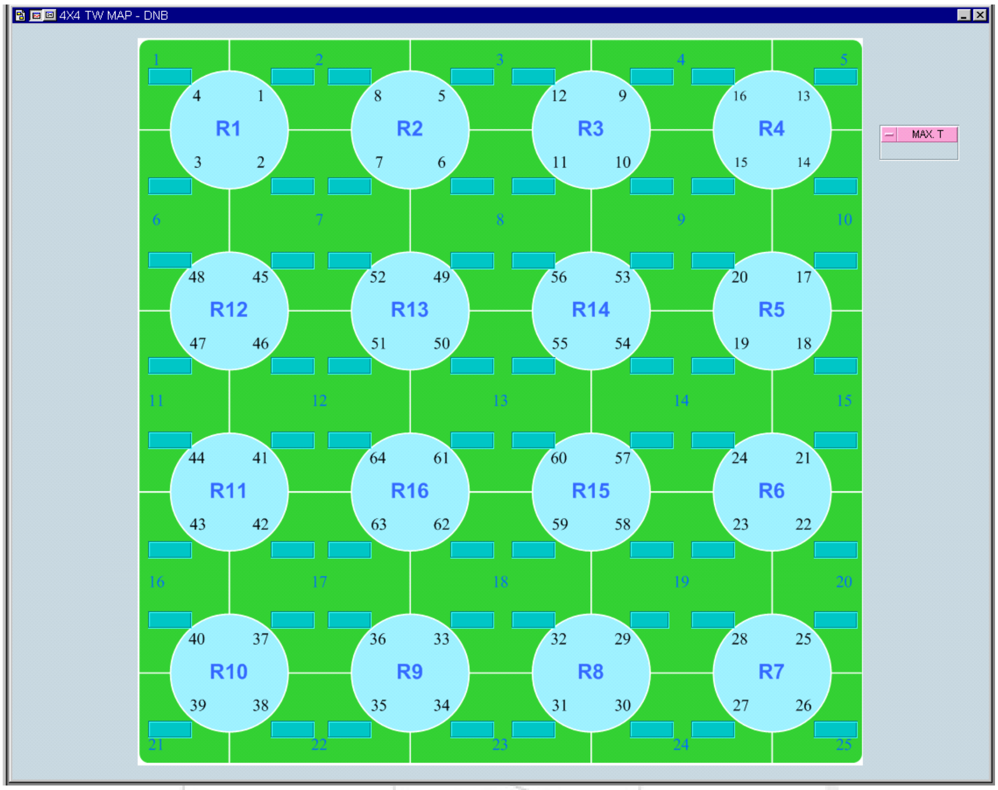


Figure 3-2. HP VEE programs showing the heater wall temperature measurements

# 4. Design Specification of Rod Bundle Test Section

Pressure vessel of the test section is made of stainless steel pipe (6 inch, Sch80) and composed of test section body, upper plenum, and lower plenum. Figure 4-1 shows the photograph of the pressure vessel outline of the test section. In the pressure vessel of the test section, shroud made of stainless steel pipe (4 inch, Sch20) and ceramic housing made of alumina are installed to form a flow channel. Figure 4-2 shows the cross-sectional view of the test section.

Test section consists of a 5x5 array of electrical heater rods. The heater rods, having the outer diameter of 9.5 mm and the heated length of 2000 mm, are made of Inconel 601 tube and directly heated by a direct-current passing through the heater wall. Axial power distribution of the heater rod is uniform. The upper end of the heater rod is screwed onto the tie-plate placed in the upper part of the pressure vessel and the lower end goes through the bottom O-ring flange to allow the heater rod to extend due to thermal expansion. The pressure boundary between heater rod and the bottom O-ring flange is maintained by the O-ring made of Teflon. A copper tie-plate acts as an electrode and is connected with bus bar. Figure 4-3 shows the photograph of copper tie-plate and bus bar. Specifications of the heater rods are summarized in Table 4-1. Table 4-2 summarizes the thermo-hydraulic and geometric data of the 5x5 rod bundle.

For measuring the heater rod wall temperature and detecting the CHF occurrence, K-type thermocouples with a sheath outer diameter of 0.5 mm are attached to the inside surface of the heater rod wall. Each of the heater rods contains four thermocouples. The temperature sensing points are located 10 mm below from the top end of the heated section, since the CHF in a vertical upward flow with an axially uniform heat flux always occurs at the top end of the heated section. Figure 4-4 shows the schematic diagram of heater rod and photograph of 5x5 rod bundle held by spacer grid.

As for the purpose of the test, the radial power distribution of the 5x5 rod bundle can be adjusted by installing the heater rods which have different electrical resistance as shown in Figure 4-5. In Figure 4-5, the power factor is defined as the ratio of the local heater rod power to the averaged heater rod power. The 5x5 heater rod array is held by Inconel spacer grids. 3 type of spacer grids having different configuration of mixing vane such as plain, split and hybrid mixing vane were used in the CHF experiments. The spacer grid locations as well as the thermocouple elevations are shown in Figure 4-6.

Figure 4-1. Photograph of the pressure vessel outline

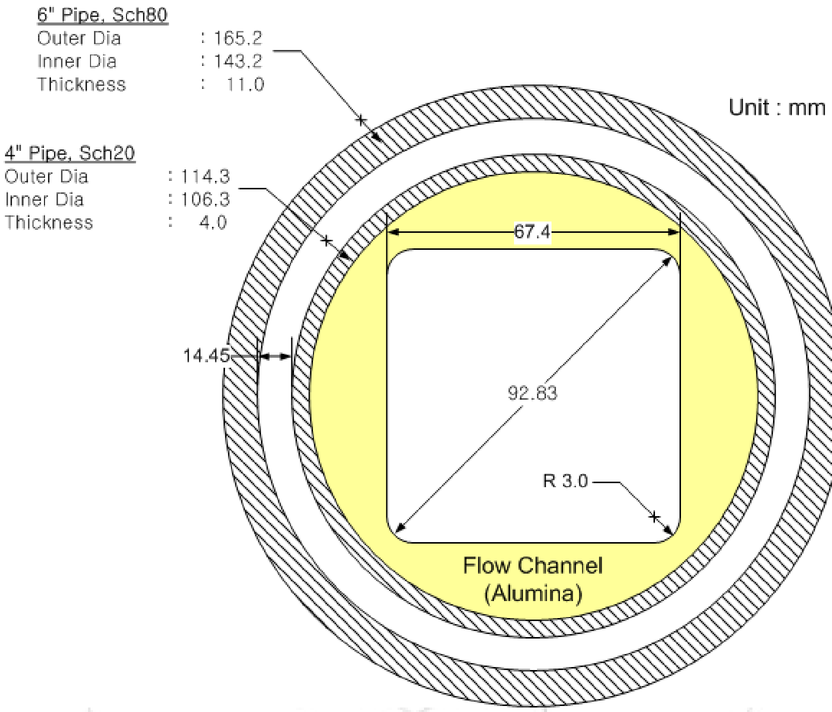


Figure 4-2. Cross-sectional view of the test section

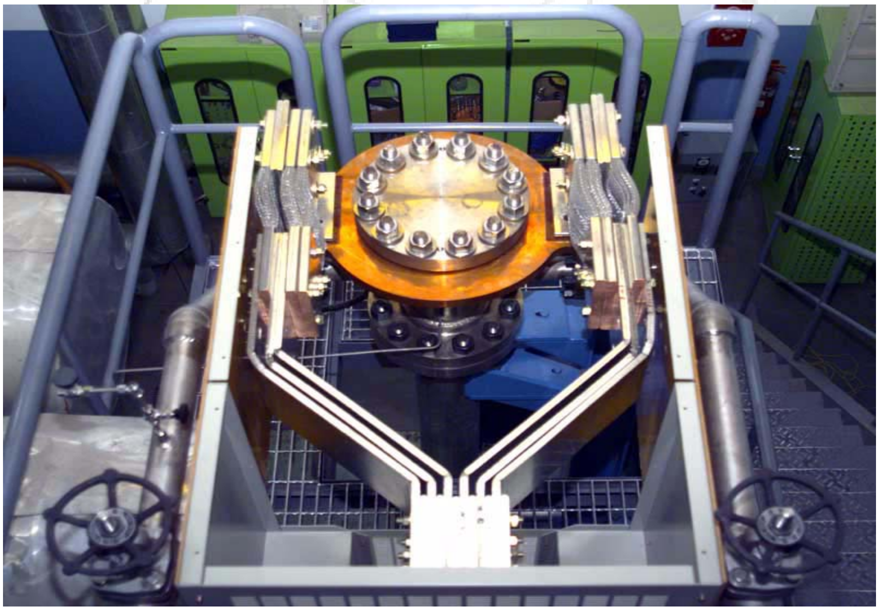

Figure 4-3. Photograph of copper tie plate and bus bar

Table 4-1. Specification of heater rods

| | | |
|---|---|---|
| A) Heater Rods | | |
| 1) Outer Diameter: | Type A (1.123 peak) | 9.50 mm ±0.05 mm |
| | Type B (0.931 peak) | 9.50 mm ±0.05 mm |
| 2) Heated Length: | Type A | 2000 mm ±1 mm |
| | Type B | 2000 mm ±1 mm |
| 3) Copper or Nickel extension | Upper Part | 500 mm ±1 mm |
| | Lower Part | 1180 ~ 1330 mm ±1 mm |
| 4) Sheath Material: | Inconel 601 | |
| B) Power Characteristics | | |
| 1) Axial Power Distribution: | Uniform | |
| 2) Radial Power Distribution: | Center 9 rods: | 1.123 ±0.03 |
| | Peripheral 16 rods: | 0.931 ±0.03 |
| 3) Heating Method: | direct heating | |
| C) Thermocouple for CHF detection | | |
| 1) Type: | K-type, ungrounded | |
| 2) Sheath Outer Diameter.: | 0.5 mm | |
| 3) Sheath Material: | Inconel | |
| 4) Number of the T/C | Type A (1.123 peak) | 4 ea (S, E, N, W) |
| | Type B (0.931 peak) | 2 ea (E, W) |

Table 4-2. Thermo-hydraulic and geometric data of the 5x5 rod bundle

| Parameter | 5X5 rod bundle |
|---|---|
| Total number of rods | 25 |
| Number of heated rods | 25 |
| Rod pitch (mm) | 12.85 |
| Rod diameter (mm) | 9.5 |
| Unheated rod diameter (mm) | N/A |
| Heated length (mm) | 2000 |
| Rod to wall gap (mm) | 3.25 |
| Corner radius (mm) | 3.0 |
| Bundle geometry data | |
| length of one-side (mm) | 67.4 |
| flow area ($mm^2$) | 2762.98 |
| wetted perimeter (mm) | 1010.58 |
| heated perimeter (mm) | 746.13 |
| hydraulic diameter (mm) | 10.94 |
| heated eqiv. diameter(mm) | 14.81 |
| Hydraulic diameter of | |
| central channel | 12.63 |
| side channel | 9.42 |
| Axial power distribution | Uniform |
| Radial power distribution | Figure 4-5 |
| Thermocouple(T/C) location | Figure 4-4 |

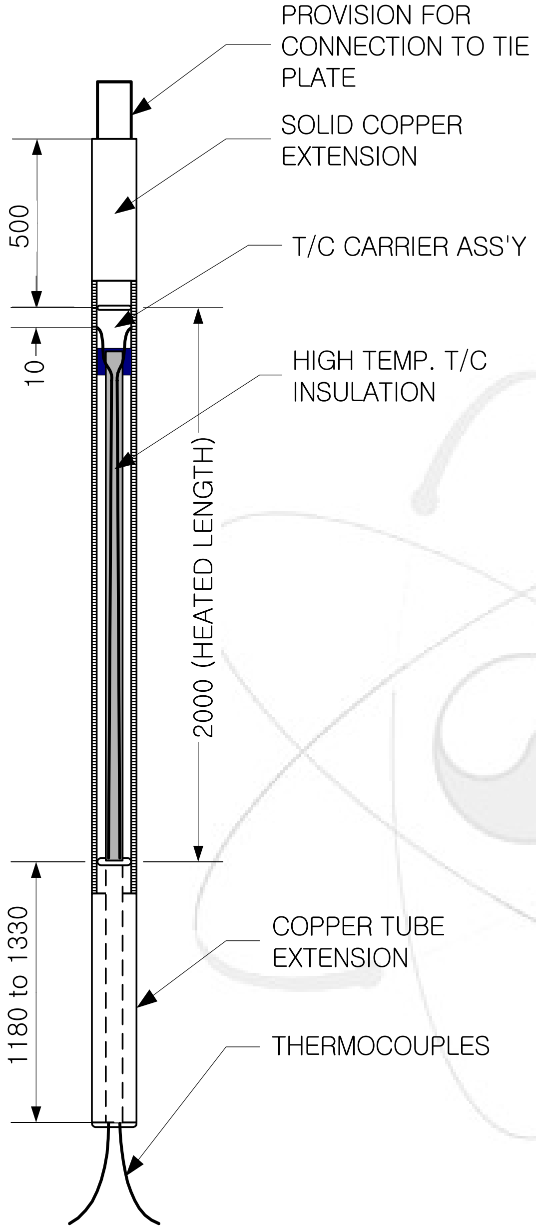


(a) Heater rod

(b) 5x5 rod bundle

Figure 4-4. Schematic diagram of heater rod and photograph of 5x5 rod bundle held by spacer grid with plain vane

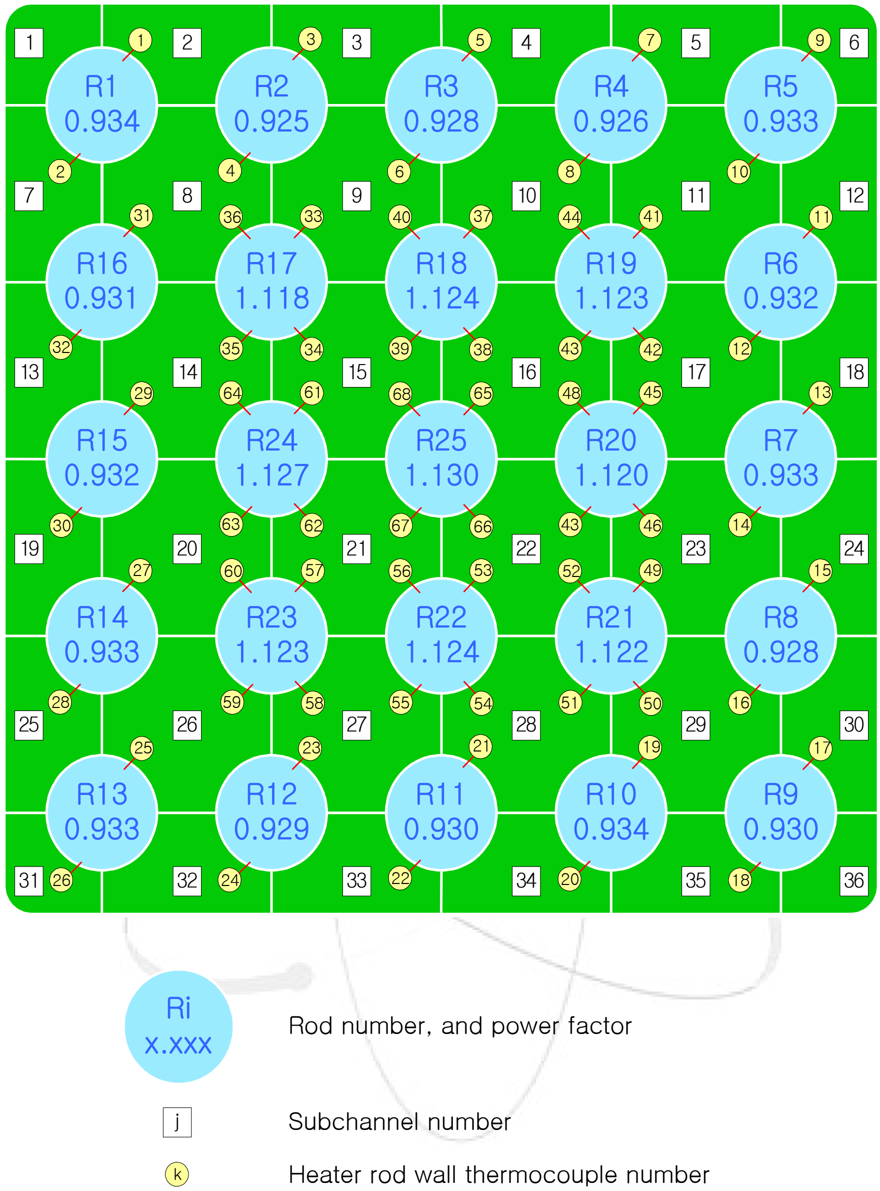


Figure 4-5. Typical example of radial power distribution of the 5x5 rod bundle

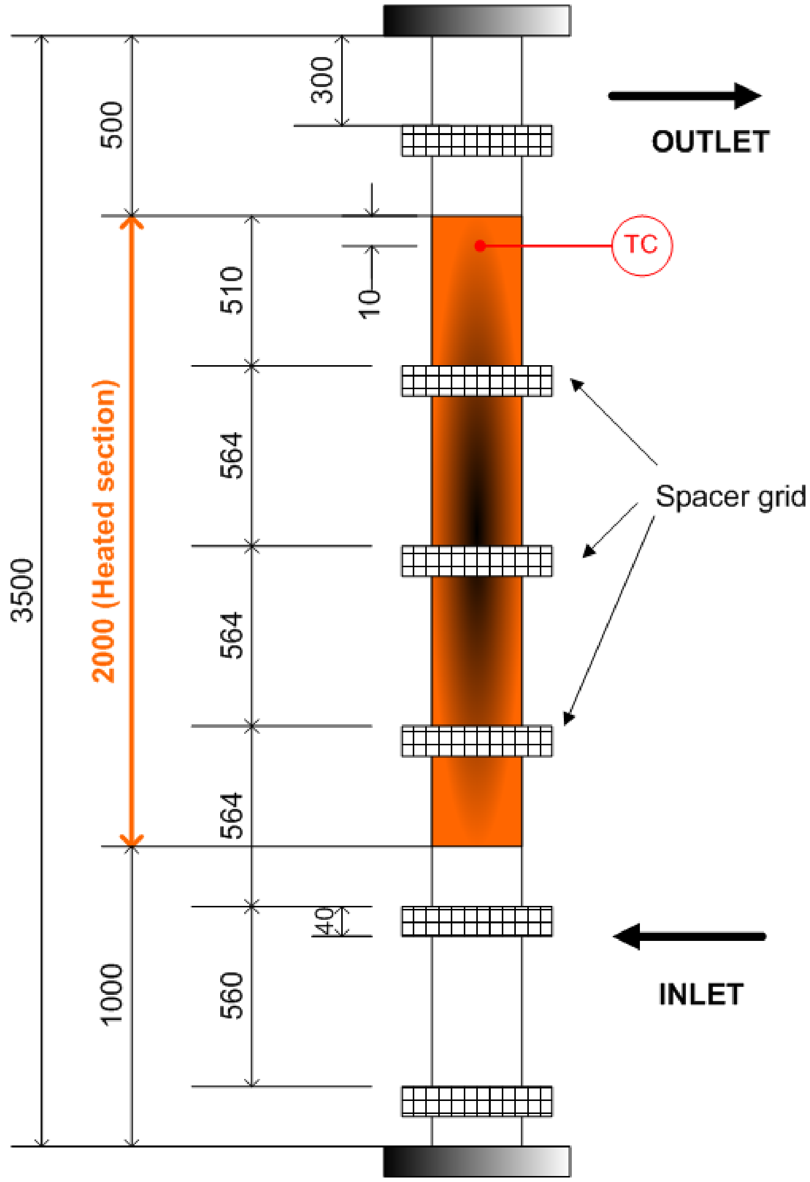


Figure 4-6. Axial locations of spacer grids and thermocouples

# 5. Experimental Work using the FTHEL

Experiments have been performed to construct the CHF data base under the various experimental conditions using the FTHEL. The primary objectives of the experiments are to investigate the CHF performance according to the design of spacer grid, the effect of unheated rods and the heat transfer characteristics at near- and supercritical pressure conditions. As for the major experimental results and findings, experimental works which have been carried out using the FTHEL are introduced in this report. Table 5-1 summarizes experimental data base which were constructed using the FTHEL facility.

Table 5-1. Experimental data base

| Experimental Conditions | | CHF | Near-critical CHF | Supercritical Heat Transfer |
|---|---|---|---|---|
| Pressure [kPa] | | 1500~3000 | 3200~4000 | 3800~4200 |
| Mass Flux [kg/m$^2$s] | | 50~3000 | 150~3000 | 150~1000 |
| Subcooling [kJ/kg] | | 10~70 | 40~70 | $T_{in}$ = 91 $^oC$ |
| Rod Array | Mixing Vane | Number of Data Base | | |
| All Heated | Plain | 218 | 220 | 50 |
| | Hybrid | 184 | 84 | 14 |
| | Split | 109 | 29 | - |
| Unheated 4EA | Plain | 194 | 80 | 62 |
| Unheated 5EA | Hybrid | 83 | 48 | 20 |
| Total Number of Data Base | | 1395 | | |

## 5.1. CHF Test under Normal Pressure Conditions

A fuel assembly of the nuclear reactors includes the spacer grids for supporting the fuel assembly. In most operating nuclear reactors, the spacer grids with mixing vanes have been adopted to improve the homogeneity of local properties inside the subchannel between the fuel rods. In this study, the systematic CHF experiments using 5x5 rod bundle haver been performed for three kinds of spacer grids, i.e., plain, split vane and hybrid vane that are developed in Korea. Parametric trends of CHF were investigated in detail.

Figure 5-1 shows the effect of mass flux on the CHF for a given pressure. For a given pressure and inlet subcooling, the effect of an increase in the mass flux is always to increase the CHF. At low mass flux below 500 kg/m$^2$s, a CHF rapidly increases with an increase of the mass flux. However, the increasing trend of a CHF with the mass flux becomes almost linear for large mass flux above 500 kg/m$^2$s. The slope of the increasing trend also becomes higher with an increase of the inlet subcooling.

Figure 5-2 shows the effect of inlet subcooling on the CHF for a given pressure of 3000 kPa. The effect of inlet subcooling on the CHF is negligible at the lowest mass flux of 50 kg/m$^2$s. However, there exists an increasing trend for the CHF with the inlet subcooling which becomes increasingly prominent for the higher mass fluxes. This trend is similar to that reported in previous study for simple geometries[3].

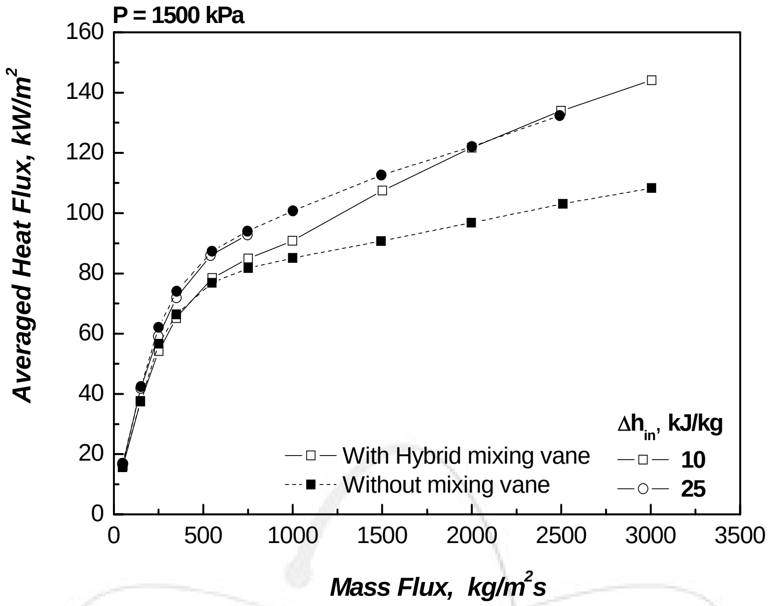


(a) P = 1500 kPa

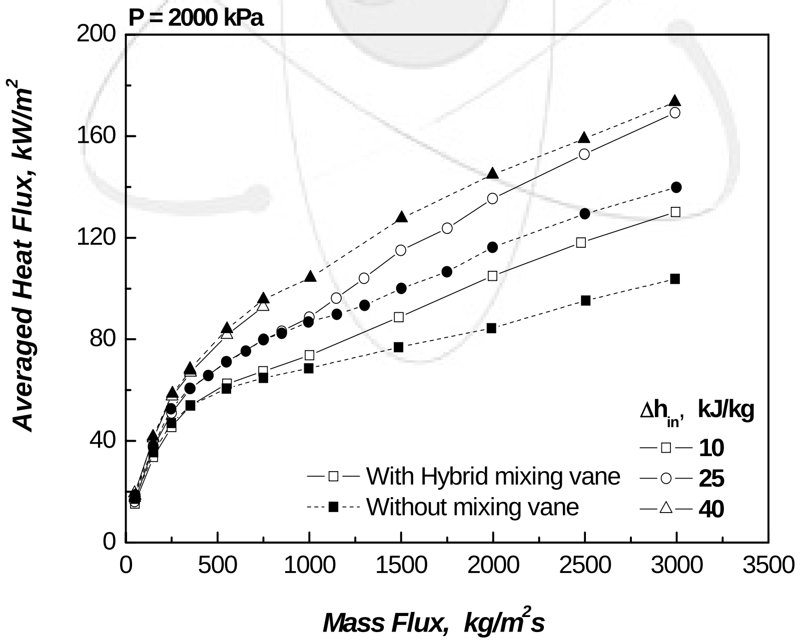


(b) P = 2000 kPa

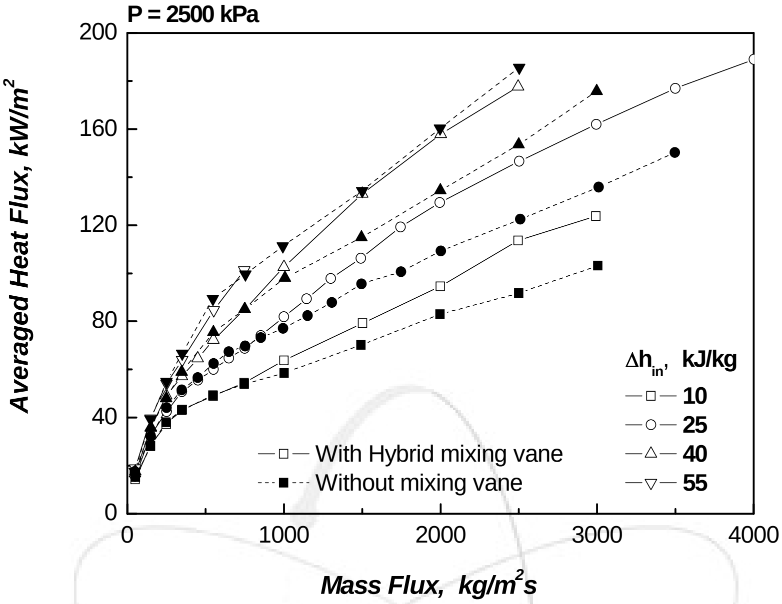


(c) P = 2500 kPa

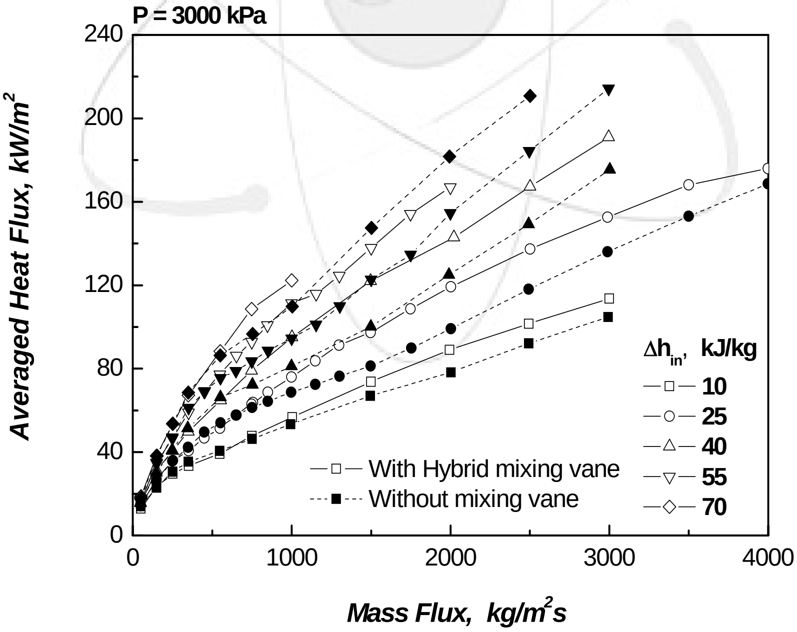


(d) P = 3000 kPa

Figure 5-1. Effect of mass flux on the CHF

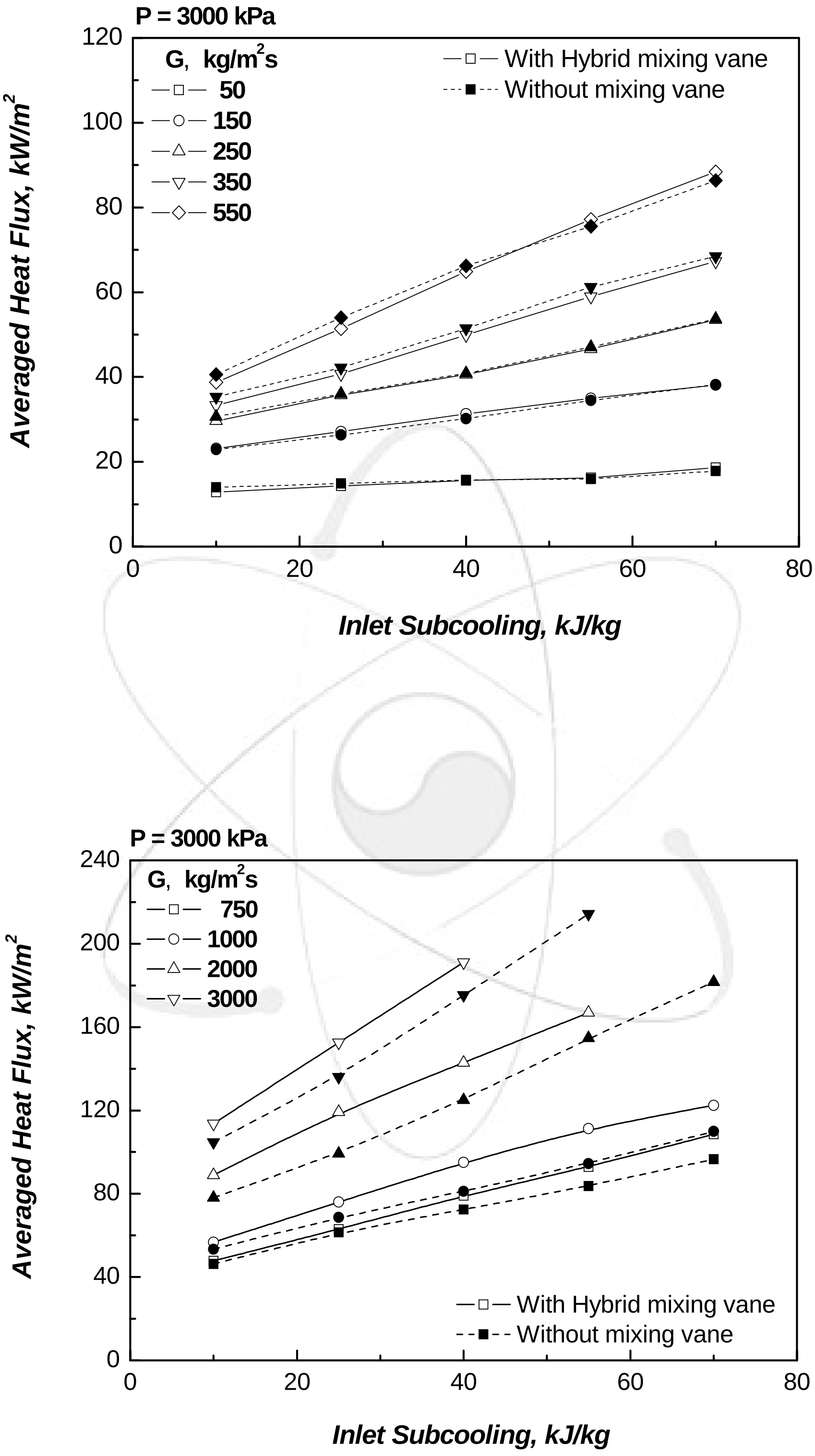


Figure 5-2. Effect of inlet subcooling on the CHF

Figure 5-3 shows the effect of exit quality on the CHF for a given mass flux and pressure. According to Figure 5-3 it can be found that only a small increase of the exit quality results in a sharp decrease on the CHF. The slope of the decreasing trend of a CHF with the exit quality is decreased for lower mass fluxes.

In general, the measured CHF data shows parametric trends for the mass flux, inlet subcooling and exit quality that are consistent with previous understandings.

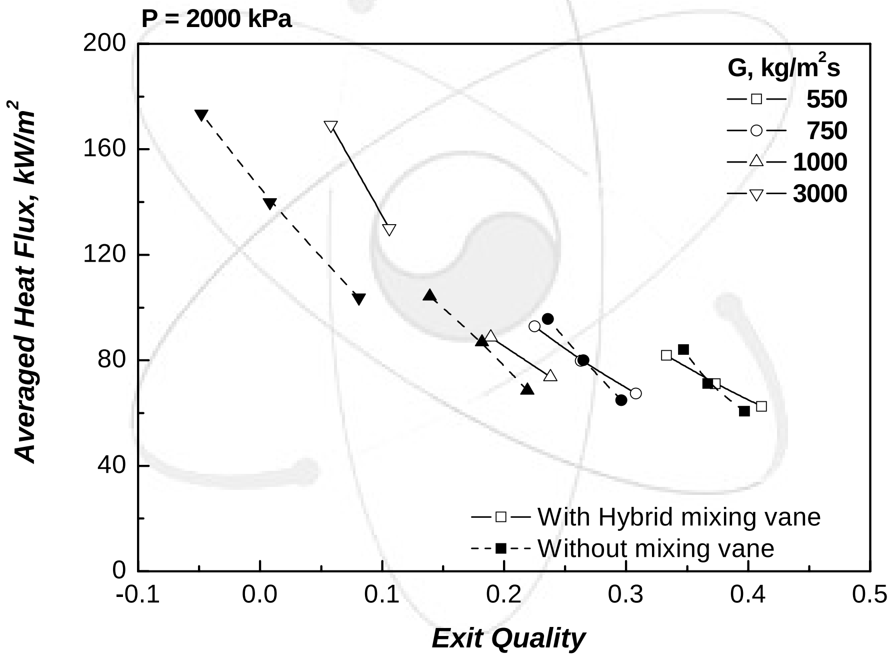


Figure 5-3. Effect of exit quality on the CHF

In this study, a CHF performance was evaluated as for the configuration of the mixing vane of the spacer grid. The measured CHF data were directly compared in both case of plain vane and hybrid mixing vane. Improvement of the CHF performance can be expressed by adopting the CHF performance factor, P. The CHF performance factor, P is defined as follows;

$$P = \frac{q''_{MV} - q''_{NMV}}{q''_{NMV}} \times 100 \qquad (5\text{-}1)$$

where, $q''_{MV}$ = CHF in case of hybrid mixing vane

$q''_{NMV}$ = CHF in case of plain vane

Figure 5-4 shows a comparison of the CHF in both case of plain vane and hybrid mixing vane. The CHF performance factor, P is about 16.4 %, which indicates that the CHF in case of hybrid mixing vane is larger than that of plain vane by 16.4 %.

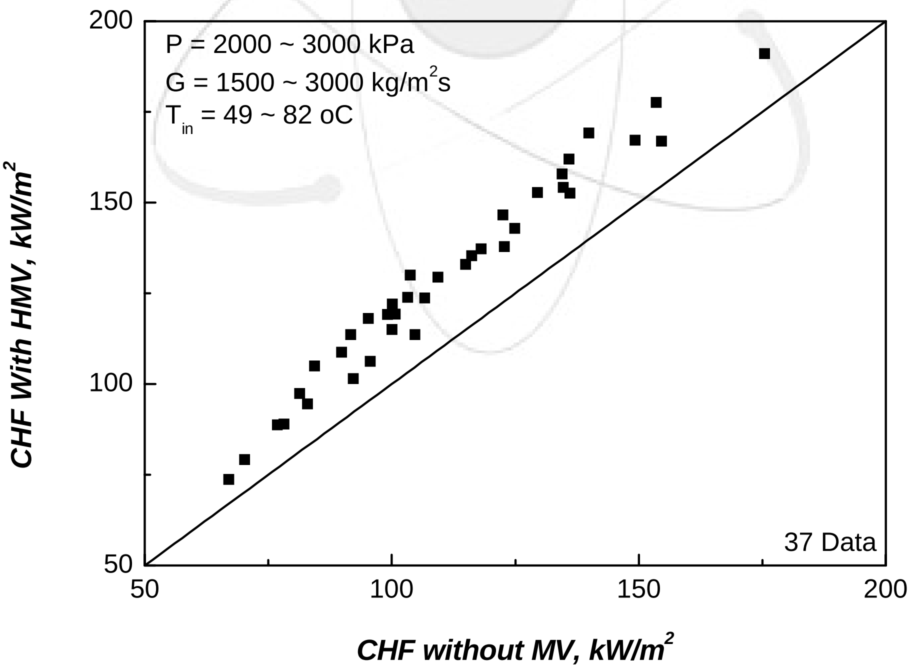


Figure 5-4. CHF Performance according to the mixing vane types

## 5.2. Thermal Mixing and Unheated Rod Effects Test

A fuel assembly of the nuclear reactors includes the unheated rods to insert control rods or in-core detectors as well as to replace damaged fuel rods during the operation. These unheated rods may change a radial power distribution and eventually affect on the local thermal hydraulic properties in the sub channels and the CHF.

Among the mathematical parameters to describe the inter-channel interactions in the rod bundle geometry, the thermal diffusion coefficient (TDC) has been used in the subchannel analysis code such as the MATRA[4] to simulate the thermal hydraulic condition of the inner-part fuel assembly of nuclear reactor. In general, the subchannel analysis code adopts the TDC to simplify the interaction between the adjacent subchannels. The accuracy of the subchannel analysis is fairly dependent on the modeling of inter-channel exchanges such as diversion cross flow and turbulent mixing. The TDC is affected by the geometry of the mixing vane and axial distances from spacer grids. Especially, turbulent mixing parameter ($\beta$) is determined considering the mixing performance of the spacer grid; it generally has the range 0.005 ~ 0.05.

In this study, single-phase thermal mixing tests were performed to find the turbulent mixing parameter. The experiments were carried out in the ranges of an outlet pressure from 2000 to 3500 kPa, a mass flux from 600 to 2500 kg/m$^2$s, an inlet coolant temperature of 50 $^o$C, and a total power of 100 and 150 kW. Local fluid temperatures in the subchannel were measured from the thermal mixing tests using the FTHEL facility and estimated from MATRA code analyses varying the turbulent mixing parameters. From this estimation, the best optimized turbulent mixing parameter was proposed for the hybrid mixing vane. The best optimized value of $\beta$ was found to be 0.02 by considering prediction statistics, i.e., average and standard deviations of the differences between the experimental results and code calculations as shown in Figure 5-5. Using the best optimized value of $\beta$ as 0.02, the MATRA predicts the test results of the fluid temperature within ±1.0 % of error as shown in Figure 5-6.

After the completion of the TDC tests, the CHF experiments were carried out to investigate the effect of unheated rods on the CHF performance. The experimental results were compared with the all heated rod bundle test results focused on the total power and the averaged heat flux at the CHF condition. The experiments were performed by maintaining the following system conditions constant: test section inlet pressure, inlet subcooling, and mass flow rate. The CHF experiments were carried out in the ranges of an outlet pressure from 2000 to 3000 kPa, a mass flux from 250 to 3000 $kg/m^2s$, an inlet subcooling from 25 to 55 kJ/kg.

Figure 5-7 shows the measured CHF data against mass flux. The experimental results were compared with the all heated rod bundle test results focused on the averaged heat flux at the CHF condition. CHF trends have two gradients with increasing the mass flux and the gradient in the low mass flux is steeper as shown in Figure 5-7. Generally, critical heat flux mechanism is classified as two different types. In the higher quality or low mass flux region, the mechanism of boiling crisis is defined as dry out resulting from a depletion of the liquid film. On the other hand, boiling crisis in the low quality or high mass flux region occurs by the transition from nucleate boiling to departure from nucleate boiling (DNB).

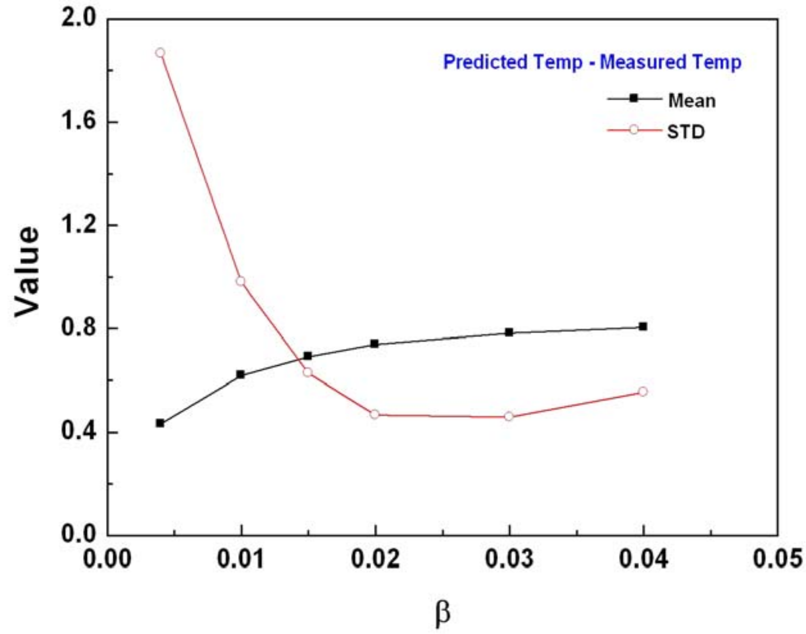


Figure 5-5. Statistics against the turbulent mixing parameter

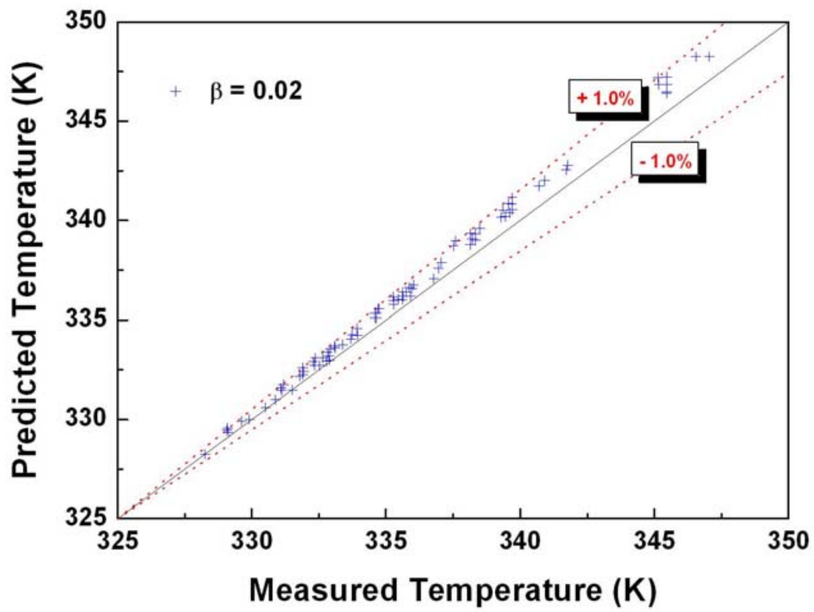


Figure 5-6. Comparison of the fluid temperatures between the measurement and MATRA prediction

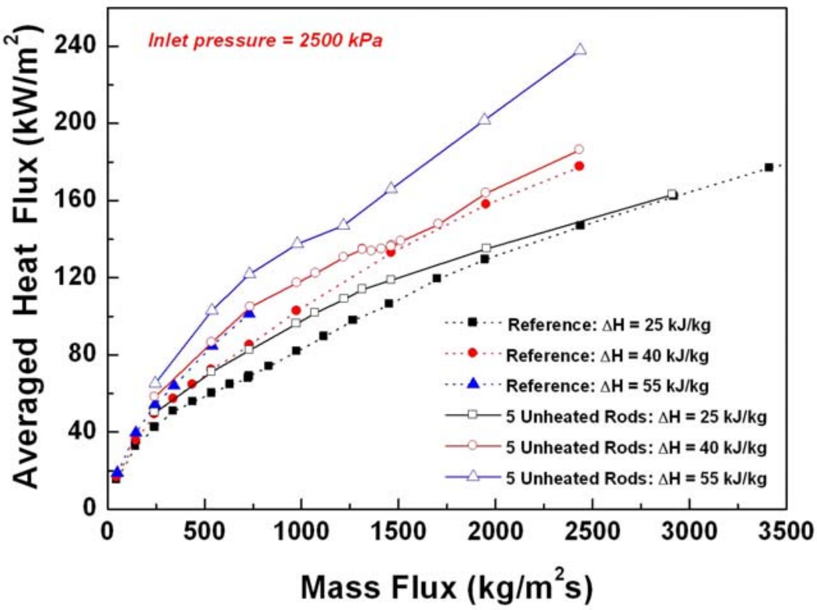


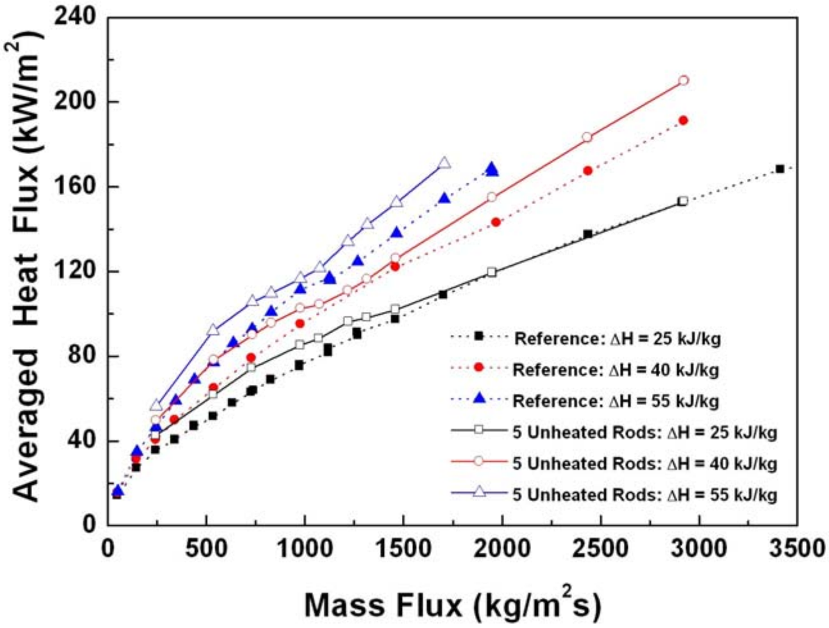


Figure 5-7. Mass flux effect on averaged heat flux at the occurrence of CHF

### 5.3. Near-Critical CHF Test and Pressure Transient Test

Super-Critical pressure Water cooled Reactor (SCWR) is considered as one of the GEN-IV (Generation IV) innovation nuclear reactors. The SCWRs, which are operated at the pressure conditions higher than the thermodynamic critical point of water (374 $^{o}$C, 22.1 MPa), have advantages over the conventional water cooled reactors in terms of a thermal efficiency as well as in compactness and simplicity[5]. The special characteristic of fluid near the thermodynamic critical point is that their thermodynamic properties vary rapidly with the temperature and pressure. A similar large variation in the fluid properties exists at a certain fluid temperature in the supercritical pressure region. The fluid temperature at which the specific heat reaches its peak value for a fixed pressure is known as the pseudo-critical point. Heat transfer to a fluid near the critical point and at supercritical pressures is characterized by such variations of the thermodynamic properties with temperature.

Since supercritical pressure fluids do not undergo a change of phase, the SCWRs at the rated operating conditions are free from the CHF-related criteria. When the SCWRs are operated with a sliding pressure start-up mode, that is, a nuclear heating starts at sub-critical pressures, a CHF should be avoided during the power-increasing phase under sub-critical pressure conditions, just as the power of Light Water Reactor (LWR) is rigidly regulated with the CHF-related criteria. Moreover, in order to ensure the reliability of safety analyses with the computer codes for abnormal pressure decreasing transients including a loss of coolant accident, it is necessary to understand the CHF characteristics near the critical pressure[5,6].

In this study, an experimental study on the CHF near the critical pressure has been performed with a 5x5 rod bundle of the FTHEL facility. Figure 5-8 shows the critical power as a function of the pressure at a fixed mass flux. The CHF decreases monotonously up to a pressure of 4.0 MPa with an increasing pressure. The decreasing rate is higher in case of high mass flux conditions. It can be speculated that the sharp decrease of the CHF might be caused by the decrease of latent heat of fluid with an increasing pressure.

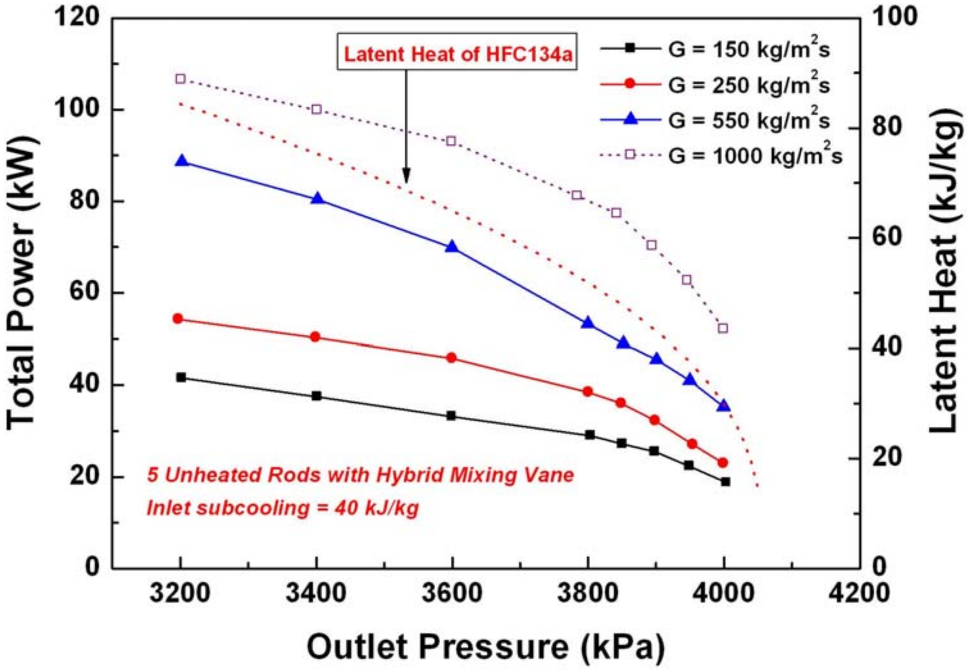


Figure 5-8. Critical power as a function of pressure at a fixed mass flux

Pressure transient experiments were performed from sub-critical pressure to supercritical pressure region. Figures 5-9 and 5-10 show the wall temperature behavior of the heater rods during pressure increase transient and pressure decrease transient, respectively. In the pressure increase transients, as the pressure approaches to critical pressure, the wall temperature increased abruptly. As soon as the pressure pass through the critical pressure, the temperature of the heater rod reduced by high heat transfer property of the supercritical fluid. The total power where the rapid wall temperature increase occurred in the pressure transient tests were similar to those of the near critical CHF tests as shown in Figure 5-11, which indicates that the rapid wall temperature increase in the pressure transient tests can be defined as CHF. In the pressure decrease transients, as soon as the pressure passes through the critical pressure from the supercritical pressure, the wall temperature rise rapidly due to the occurrence of the CHF.

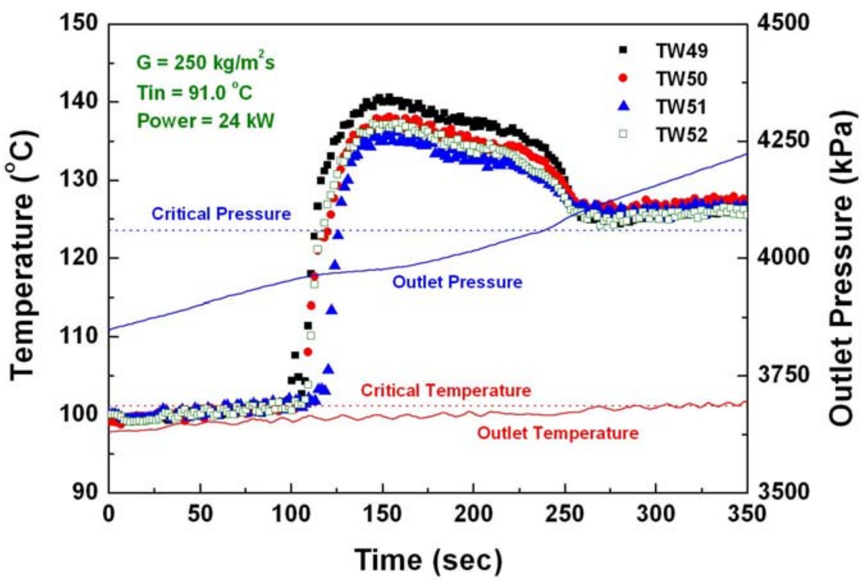


Figure 5-9. Wall temperature behavior during pressure increase transient

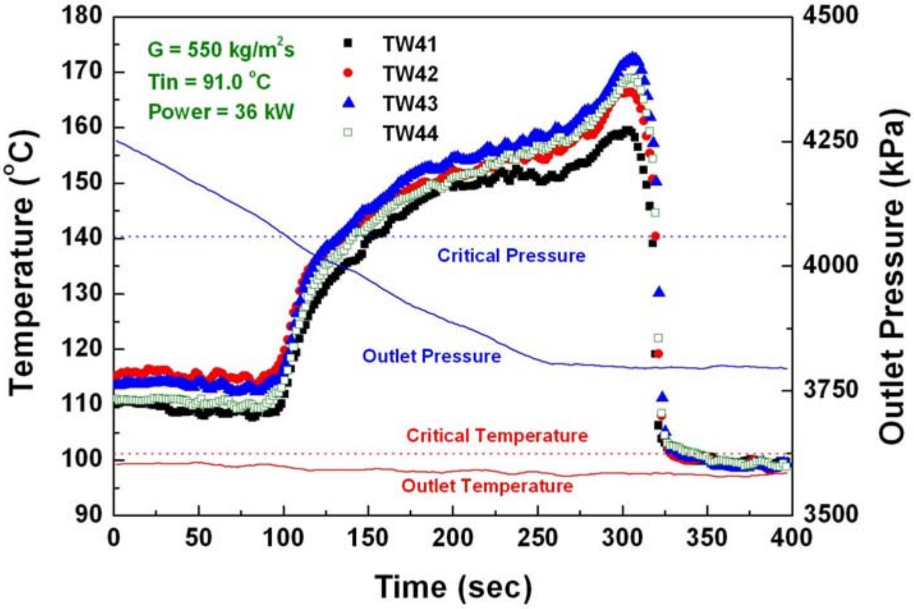


Figure 5-10. Wall temperature behavior during pressure decrease transient

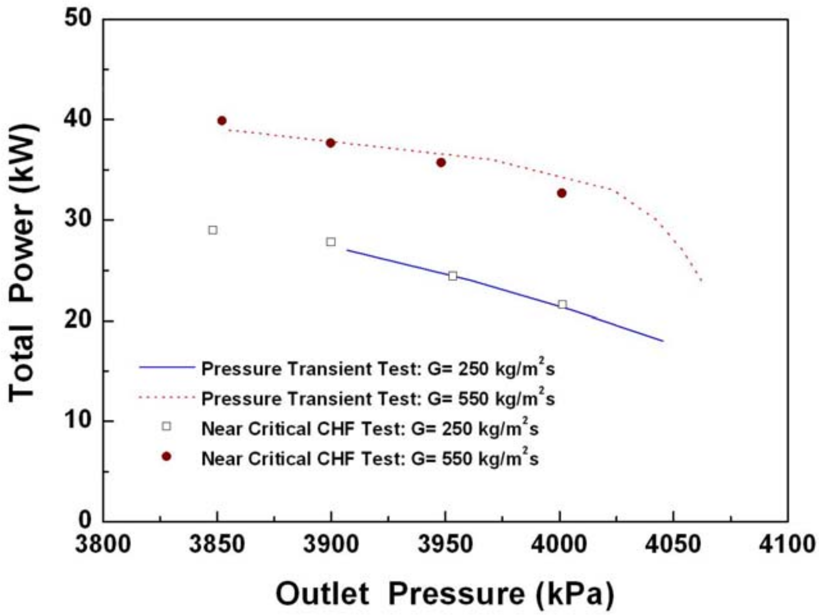


Figure 5-11. Comparison of CHF data with the onset of heat transfer deterioration during pressure transients

# 6. Conclusions

In this report, detailed design specification of the Freon Thermal Hydraulic Experimental Loop (FTHEL) facility and its application are summarized. The FTHEL is used to investigate a thermal mixing and a critical heat flux (CHF) performance in 5x5 rod bundles. The Freon, HFC-134a, is used as working fluid medium. The FTHEL consists of a closed hydraulic loop with main circulation pumps, pre-heaters, test section, direct current (DC) power supply, condensers and coolers. The system was designed with operating limits of 4.5 MPa and 150 $^{o}$C.

A series of experiments have been performed to construct the CHF data base under the various experimental conditions using the FTHEL. The primary objectives of the experiments are to investigate the CHF performance according to the design of spacer grid, the effect of unheated rods and the heat transfer characteristics at near- and supercritical pressure conditions. Recently, the FTHEL facility is being used for the CHF experiments which are organized to support the development of improved spacer grid by the domestic and the foreign nuclear fuel companies.

## References


[1] Se-Young Chen et al., "Comparison of the CHF data for water and refrigerant HFC-134a by using the fluid-to-fluid modeling methods," Int. J. Heat and Mass Transfer **50**, pp. 4446 ~ 4456 (2007).

[2] International Organization for Standardization (ISO), Guide to the Expression of Uncertainty in Measurement, ISBN 92-67-10189-9 (1995).

[3] C. F. Fighetti et al., Parametric Study of CHF Data Volume 1, Compilation of Rod Bundle CHF Data available at the Columbia University Heat Transfer Research Facility, EPRI Report NP-2609, **1**, (1982).

[4] Y. J. Yoo et al., Development of a Subchannel Analysis Code MATRA (Verv. a), KAERI/TR-1033/98 (1998).

[5] Y. Oka, "Research and development of the supercritical-pressure light water cooled reactors," Proc. 10th Int. Topical Meeting on Nuclear Reactor Thermal Hydraulics (NURETH-10), Seoul, Korea, Paper KL-02 (2003).

[6] Se-Young Chun et al., "Critical Heat Flux in a Heater Rod Bundle Cooled by R-134a Fluid near the Critical Pressure," J. of Nuclear Science and Technology, **44**, No. 9, pp. 1189 ~ 1198 (2007).

서 지 정 보 양 식

| 수행기관보고서번호 | 위탁기관보고서번호 | 표준보고서번호 | INIS 주제코드 |
|---|---|---|---|
| KAERI/TR-3592/2008 | | | |

| | |
|---|---|
| 제목 / 부제 | 프레온 열수력 실험장치의 계통 설명 및 활용 |
| 연구책임자 및 부서명<br>(AR,TR 등의 경우 주저자) | 강 경 호 (열수력안전연구부) |
| 연 구 자 및 부 서 명 | 추연준, 윤영중, 박종국, 김복득, 문상기, 천세영, 송철화, 백원필<br>(열수력안전연구부), 신창환(선진핵연료기술개발부) |

| | | | | | |
|---|---|---|---|---|---|
| 출 판 지 | 대전 | 발행기관 | 한국원자력연구원 | 발행년 | 2008. 6 |
| 페 이 지 | p.56 | 도 표 | 있음( ○ ), 없음( ) | 크 기 | 21x29Cm. |
| 참고사항 | | | | | |
| 공개여부 | 공개( ○ ), 비공개( ) | | 보고서종류 | 기술보고서 | |
| 비밀여부 | 대외비( ), __ 급비밀 | | | | |
| 연구위탁기관 | | | 계약번호 | | |


초록 (15-20줄내외)

한국원자력연구원에서는 프레온 열수력 실험 장치(FTHEL: Freon Theraml Hydraulic Experimental Loop)를 운영하고 있다. 프레온 열수력 실험 장치는 프레온 냉매(HFC-134a)를 사용하여 5x5 봉다발에서 열혼합과 임계열유속(CHF: Critical Heat Flux) 성능 평가를 위한 실험 수행에 활용된다. 프레온 열수력 실험 장치는 주냉각펌프, 가압기, 예열기, 시험대, 응축기 및 열교환기로 구성되어 있다. 실험 장치는 스테인레스 스틸로 제작되었으며, 실험 장치의 최대 운저 허용 압력과 온도는 각각 4.5 MPa, 150 $^{o}$C이다. 주냉각재 펌프는 non-seal canned motor 펌프로서 펌프 두 대를 직렬로 설치하여 100m의 최대 수두로 냉각재를 순환시킨다. 계통 압력은 질소 가스를 사용하는 accumulator를 이용하여 제어한다. 예열기는 시험대의 입구온도를 조절하는 장치이며, 응축기는 시험대에서 생성된 증기를 응축하는 장치로서 쉘튜브형의 개별 응축기의 용량은 40 kW로 두 개를 사용하여 총 용량은 80 kW이다. 시험대에서 가열된 냉각수를 냉각시켜 시험대 입구에서의 유체온도를 일정하게 유지시키기 위한 열교환기는 두 대가 병렬로 설치되어 있으며, 열전달 조절 범위를 넓히기 위하여 우회 유로를 설치하였다. 프레온 열수력 실험 장치의 전원 공급 장치는 전압이 최고 60 V까지 공급되고 전류는 최고 12000 A까지 제공되는 직류전원 장치이다.

프레온 열수력 실험 장치를 이용하여 광범위한 실험 조건에서 임계열유속 데이터베이스를 구축하기 위한 실험을 수행하였다. 지지격자의 형상에 따른 임계열유속의 특성과 성능평가를 위한 실험을 수행하였으며, 5x5 봉다발 내에 비가열봉을 삽입하여 비균일 출력분포 효과에 대한 특성 실험 및 초임계압 근처 임계열유속 실험과 초임계압 압력 천이 열전달 실험을 수행하여 다양한 원자로 운전 조건에 대한 임계열유속과 열전달 특성을 분석하였다.


| | |
|---|---|
| 주제명키워드<br>(10단어내외) | 임계열유속, 프레온 열수력 실험장치, 봉다발 |

<table>
<tr><td colspan="8">BIBLIOGRAPHIC INFORMATION SHEET</td></tr>
<tr><td>Performing Org.<br>Report No.</td><td colspan="2">Sponsoring Org.<br>Report No.</td><td colspan="3">Stamdard Report No.</td><td colspan="2">INIS Subject Code</td></tr>
<tr><td>KAERI/TR-3592/2008</td><td colspan="2"></td><td colspan="3"></td><td colspan="2"></td></tr>
<tr><td>Title / Subtitle</td><td colspan="7">Description of Freon Thermal Hydarulic Experimental Loop (FTHEL) and its Application</td></tr>
<tr><td>Project Manager and Department (or Main Author)</td><td colspan="7">Kyoung-Ho Kang</td></tr>
<tr><td>Researcher and Department</td><td colspan="7">Chang-Hwan Shin, Yeon-Jun Choo, Young-Jung Youn, Jong-Kuk Park, Bok-Deuk Kim, Sang-Ki Moon, Se-Young Chun, Chul-Hwa Song, Won-Pil Baek</td></tr>
<tr><td>Publication Place</td><td>Daejeon</td><td>Publisher</td><td colspan="2">KAERI</td><td>Publication Date</td><td colspan="2">2008.6</td></tr>
<tr><td>Page</td><td>p.56</td><td>Ill. & Tab.</td><td colspan="2">Yes(○), No ( )</td><td>Size</td><td colspan="2">21x29 Cm.</td></tr>
<tr><td>Note</td><td colspan="7"></td></tr>
<tr><td>Open</td><td colspan="2">Open(○), Closed( )</td><td rowspan="2" colspan="2">Report Type</td><td rowspan="2" colspan="3"></td></tr>
<tr><td>Classified</td><td colspan="2">Restricted( ), ___Class Document</td></tr>
<tr><td>Sponsoring Org.</td><td colspan="2"></td><td colspan="2">Contract No.</td><td colspan="3"></td></tr>
<tr><td colspan="8">Abstract (15-20 Lines)<br><br>Freon Thermal Hydraulic Experimental Loop (FTHEL) is being operated at the Korea Atomic Energy Research Institute (KAERI). The FTHEL is used to investigate a thermal mixing and a critical heat flux (CHF) performance in 5x5 rod bundles. The Freon, HFC-134a, is used as working fluid medium. The FTHEL consists of a closed hydraulic loop with main circulation pumps, pre-heaters, test section, direct current (DC) power supply, condensers and coolers. The system was designed with operating limits of 4.5 MPa and 150 $^{o}$C. Flow in the loop is provided by two non-seal canned motor pumps in a series arrangement. The series arrangement of the main circulation pumps provides a total developed head of 100 m. System pressure is controlled by accumulator using compressed nitrogen gas as working fluid. A pair of pre-heaters adjusts the inlet temperature of fluid at the test section. The vapor generated in the test section is condensed in the shell-tube type condensers and cooled in the same type coolers. The power to the test section is supplied from a 60 V x 12000 A, DC source.<br><br>Experiments have been performed to construct the CHF data base under the various experimental conditions using the FTHEL. The primary objectives of the experiments are to investigate the CHF performance according to the design of spacer grid, the effect of unheated rods and the heat transfer characteristics at near- and supercritical pressure conditions.</td></tr>
<tr><td>Subject Keywords (About 10 words)</td><td colspan="7">CHF, FTHEL, Rod bundle, HFC-134a</td></tr>
</table>